scientific reports

OPEN

Plastome phylogenomics of the Korean endemic plant *Arisaema thunbergii* subsp. *geomundoense* (Araceae)

Joonhyung Jung[1,2]✉, Suvin Seok[3], Hye One Kim[4], Kashish Kamra[4], Hyuk-Jin Kim[2] & Joo-Hwan Kim[4]✉

Studying endemic plants is crucial for enhancing biodiversity in their unique habitats and exploring their evolutionary history. However, classification relying only on morphological traits can be subjective and may lead to inconsistencies in taxonomy. To address this issue, molecular approaches are necessary for precise identification and classification. The Korean endemic plant *Arisaema thunbergii* Blume subsp. *geomundoense* S.C.Ko (Araceae Juss.) has been classified based on its distinct spadix appendage color and wrinkled texture. Nevertheless, its taxonomic placement remains uncertain owing to a lack of sufficient molecular research, and it has recently been treated as a synonym of *A. thunbergii* subsp. *urashima* (H.Hara) H.Ohashi & J.Murata. To resolve their evolutionary relationships, we sequenced and analyzed the complete plastid genomes of *A. thunbergii* subsp. *geomundoense*, *A. thunbergii* subsp. *thunbergii* and *A. heterophyllum* Blume, obtaining genome lengths of 168,650–173,154 bp. Each plastome harbors 78 protein-coding genes (PCGs), 30 tRNA genes, and four rRNA genes, with *inf*A retained as a pseudogene. Phylogenetic reconstruction based on all 78 plastid PCGs robustly supports the monophyly of seven of the 15 recognized sections in *Arisaema* Mart. and confirm that *A. thunbergii* subsp. *geomundoense* is nested within *A. thunbergii* subsp. *thunbergii*. Based on these findings, we propose that *A. thunbergii* subsp. *geomundoense* should be treated as a synonym of *A. thunbergii* subsp. *thunbergii*. Molecular clock estimates indicate that *Arisaema* first appeared in the Oligocene and subsequently radiated during the Miocene. Utilizing plastome sequences and previously established calibration points, this study refines the evolutionary timeline of *Arisaema*, highlighting its divergence and adaptation during the Miocene.

Keywords Korean endemic plant, *Arisaema thunbergii* subsp. *geomundoense*, Plastid genome (plastome), Phylogenetic analyses, Divergence times, Taxonomic treatment

Endemic plants are species native exclusively to a specific region. These plants have evolved by adapting to unique ecological and geographical characteristics, possessing genetic diversity that is essential for understanding their evolution, speciation, and biogeography[1,2]. In the Korean Peninsula, Nakai[3] initially cataloged 1,118 endemic vascular plant taxa. However, subsequent studies later revised and refined these records, excluding cultivated varieties from their assessments, ultimately identifying 373 endemic taxa[4–9]. Despite the recognition of newly identified endemic taxa in Korea, considerable confusion remains due to ongoing debates over scientific nomenclature and the taxonomic validity of certain taxa.

Araceae Juss., primarily distributed in temperate and tropical regions, comprise approximately 143 genera and over 3,600 species, characterized by inflorescences forming a spadix-spathe pseudanthium[10,11]. The family has been classified into multiple subfamilies, with Mayo et al.[10] recognizing seven subfamilies. Later, Bogner and Hesse[12] proposed the addition of the subf. Zamioculcadoideae. Phylogenetic analyses have supported this classification[13–16]and recent studies have confirmed an eight-subfamily classification, despite ongoing taxonomic disagreements[16]. Among the genera of the subf. Aroideae, *Arisaema* Mart., commonly known as

[1]Division of Botany, Honam National Institute of Biological Resources, 99 Gohadoan-gil, Mokpo-si, Jeollanam-do, Republic of Korea. [2]Division of Forest Biodiversity, Korea National Arboretum, 509 Gwangneungsumogwon-ro, Pocheon-si, Gyeonggi-do, Republic of Korea. [3]Department of Life Science, Hanyang University, 222 Wangsimni-ro, Seoul, Republic of Korea. [4]Department of Life Sciences, Gachon University, 1342 Seongnam-daero, Seongnam-si, Gyeonggi-do, Republic of Korea. ✉email: joonhyung0104@gmail.com; kimjh2009@gachon.ac.kr

the cobra Lily, comprises approximately 212 species of perennial herbs found in forests. It has been widely studied for its bioactivity properties, including antioxidant, anticancer, insecticidal, antimicrobial, anthelmintic, and hepatoprotective effects[17]. With respect to the previously diverse infrageneric classification systems of *Arisaema*, Murata et al.[18] proposed 14 sections in their nomenclatural review, while Ohi-Toma et al.[19], based on phylogenetic analyses, identified 15 sections and further refined species-level classifications. In Korea, both *A. takesimense* Nakai and *A. thunbergii* Blume subsp. *geomundoense* S.C.Ko are recognized as endemic plants[9]. The latter subspecies was first described from Geomundo Island, part of Dadohaehaesang National Park, and was initially classified within section *Tortuosa* subsect. *Flagellarisaema*, now recognized as sect. *Flagellarisaema*[20]. It has drawn academic interest due to its distinctive ecological adaptations. Ko et al.[20] identified the diagnostic characteristics of *A. thunbergii* and its subspecies, noting that *A. thunbergii* subsp. *geomundoense* has one or two leaves and a dark to bright purple, wrinkled spadix appendage (Fig. 1).

However, classification based solely on morphological traits may lead to subjective interpretations, highlighting the need for objective analyses using quantifiable data. Renner et al.[21] analyzed 81 taxa based on the *trn*L–*trn*F region and identified sect. *Tortuosa* as the basal lineage of the genus. Later, Ohi-Toma et al.[19] expanded upon this phylogenetic framework by incorporating four plastidial non-coding regions, further

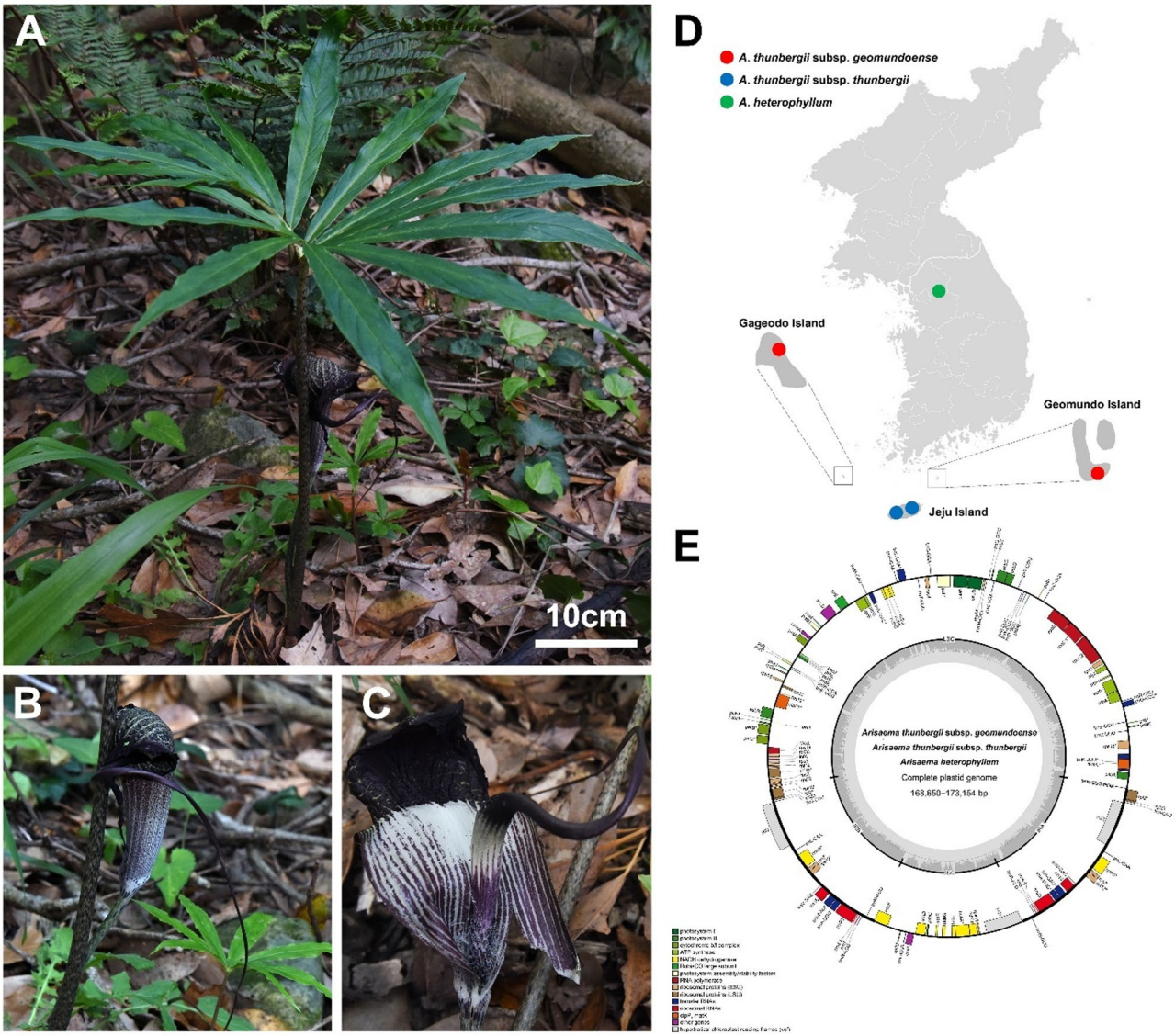

Fig. 1. Photographs of *A. thunbergii* subsp. *geomundoense*, study sampling sites, and complete plastome map of *Arisaema* taxa analyzed in this study. (**A**) Habit of the perennial plant; (**B**) Inflorescence; (**C**) Spathe and male spadix; (**D**) Map of sampling locations. The photographs were taken by Joonhyung Jung on 18 May 2022 at Mt. Suwol, Geomundo Island, Samsan-myeon, Yeosu-si, Jeollanam-do, South Korea; (**E**) Colored boxes indicate conserved plastid genes; those on the inner circle are transcribed clockwise, while those on the outer circle are transcribed counterclockwise. The innermost ring displays gray bar graphs representing the plastome's GC content.

refining the infrageneric classification of *Arisaema*. Additionally, genetic analysis of Korean *Arisaema* species based on the nuclear ITS region and the plastidial *mat*K and *rbc*L genes revealed no significant genetic differences between *A. thunbergii* subsp. *geomundoense* and *A. thunbergii* subsp. *thunbergii*[22]. In recent years, plastid genome (plastome) sequencing has become a valuable tool for studying evolutionary relationships among species. Given the highly conserved nature of plastomes, structural variations, phylogenetic analyses, and biogeographical studies have been widely used to explore angiosperm evolution[23–26]. Although recent studies on *Arisaema* have reported complete plastome sequences[27–29]structural analyses remain lacking. In addition, *A. thunbergii* subsp. *geomundoense* requires further investigation of its subspecific relationships due to insufficient genetic data. This study aims to determine the taxonomic status of *A. thunbergii* subsp. *geomundoense* as a Korean endemic plant and clarify its phylogenetic position. To achieve this, we assembled the plastomes of *A. thunbergii* subsp. *geomundoense* from two different sites along with its close relatives, *A. thunbergii* subsp. *thunbergii* and *A. heterophyllum*. Additionally, we examined plastome structural variations within the genus *Arisaema* and estimated divergence times to provide insights into its evolutionary history. Our findings will enhance the understanding of phylogenetic relationships within *Arisaema* and contribute to the conservation and clarification of the taxonomic identity of Korean endemic plants.

Results

Plastome characteristics and comparative analyses

The five plastomes analyzed in this study ranged from 168,650 base pairs (bp) in *A. heterophyllum* to 173,154 bp in *A. thunbergii* subsp. *thunbergii* (Fig. 1; Table 1). Each genome contained a total of 130 genes, including those duplicated in the inverted repeat (IR) regions. These comprised 46 RNA genes, 49 protein-coding genes (PCGs), 25 ribosomal protein genes, and 10 transcription/translation-related genes (Table S1). In the plastomes of *A. thunbergii* subsp. *geomundoense* and its close relatives within *Arisaema*, the *inf*A gene was identified as a pseudogene. The GC content varied slightly between *A. thunbergii* subsp. *geomundoense* and *A. thunbergii* subsp. *thunbergii*, ranging from 34.2 to 34.3%, indicating a highly conserved genomic structure (Table 1). The analysis revealed that the nucleotide sequences of plastid PCGs were identical between *A. thunbergii* subsp. *geomundoense* from Geomundo Island and two individuals of *A. thunbergii* subsp. *thunbergii*, confirming the absence of genetic differences. While plastid PCGs were well conserved across taxa, non-coding regions exhibited high variability (Figs. 2 and 3). No genomic inversions were detected in this study. The boundaries of the large single-copy (LSC), small single-copy (SSC), and inverted repeat (IR) regions were compared, specifically at the LSC/IRb (JLB), IRb/SSC (JSB), SSC/IRa (JSA), and IRa/LSC (JLA) junctions (Fig. 4A). Notably, the *trn*H-GUG gene was found within the boundary of the IR and LSC regions in all species except *A. ringens* (Thunb.) Schott (Fig. 4A). At the JSB, the *ndh*F gene is predominantly nested across most *Arisaema* species. However, *A. flavum* (Forssk.) Schott and *A. ringens* exhibit a distinct pattern, with *ndh*F located exclusively within the SSC region. No other notable structural characteristics were observed at the respective region boundaries.

We assessed nucleotide diversity (*Pi*) across 15 *Arisaema* taxa (Fig. 4B and Table S2). For plastid PCGs, *Pi* values spanned from 0 (*atp*H, *pbf*1, *pet*G, *pet*L, *pet*N, *psa*J, *psb*F, *psb*I, and *psb*T) to 0.01287 (*ycf*1), averaging 0.0038. Among tRNA and rRNA genes, eleven loci showed variation, with *Pi* ranging from 0.00365 (*trn*F-GAA) to 0.03411 (*rrn*23) and a mean of 0.0035. In contrast, for the standard deviation of *Pi*, among the plastid PCGs, *psa*I exhibited the highest value at 0.00554 (mean 0.00083), while among the tRNA and rRNA genes, *trn*H-GUG and *rrn*23 showed the highest values at 0.01111 and 0.02865, respectively. In the intergenic spacers (IGS), the *trn*N-GUU–*ndh*F region exhibited the highest *Pi* at 0.05842, whereas the *ndh*A–*ndh*H, *psa*B–*psa*A, *psb*F–*psb*E, *psb*L–*psb*F, *rpl*2–*rpl*23, *rpo*C1–*rpo*B, *rps*7–*rps*12, *rrn*4.5–*rrn*5, *trn*I-CAU–*ycf*2, and *trn*I-GAU–*trn*A-UGC regions all had *Pi* values of 0; the standard deviation of *Pi* was highest in the *rrn*23–*rrn*4.5 spacer at 0.03593.

Codon usage in *Arisaema*

Relative synonymous codon usage (RSCU) was assessed for 78 plastid PCGs across *Arisaema* taxa (Fig. 5). Stop codons (UAA, UAG, and UGA) were excluded from this evaluation. The dataset comprised between 22,667 and 22,759 codons (Table S3). Among amino acids, leucine (L) was the most abundant amino acid (10.28–10.30%), while cysteine (C) was the least represented (1.12–1.15%) (Table S3). In terms of codon preference, AUU (coding

Taxa	Length and G + C content				GenBank accession No.	Voucher
	LSC bp (G + C%)	SSC bp (G + C%)	IR bp (G + C%)	Total bp (G + C%)		
Arisaema thunbergii Blume subsp. *geomundoense* S.C.Ko (Geomundo Island)	96,154 (32.3)	23,136 (27.5)	26,570 (40.9)	172,430 (34.3)	PV231678	JH220518001
Arisaema thunbergii Blume subsp. *geomundoense* S.C.Ko (Gageodo Island)	96,574 (32.2)	23,144 (27.5)	26,599 (40.8)	172,916 (34.2)	PV231677	JH220506001
Arisaema thunbergii Blume subsp. *thunbergii* (Gyoraeri Natural Recreation Forest, Jeju Island)	96,893 (32.4)	23,139 (27.5)	26,561 (40.9)	173,154 (34.3)	PV231679	JH220519001
Arisaema thunbergii Blume subsp. *thunbergii* (Seogwipo Natural Recreation Forest, Jeju Island)	96,325 (32.3)	23,150 (27.5)	26,570 (40.9)	172,615 (34.3)	PV231680	JH220519005
Arisaema heterophyllum Blume (Mt. Cheonggye)	93,976 (32.8)	22,140 (28.3)	26,267 (41.3)	168,650 (34.9)	PV231676	JH220531001

Table 1. Characteristics of the large single-copy (LSC), small single-copy (SSC), and inverted repeat (IR) regions in the plastomes analyzed in this study.

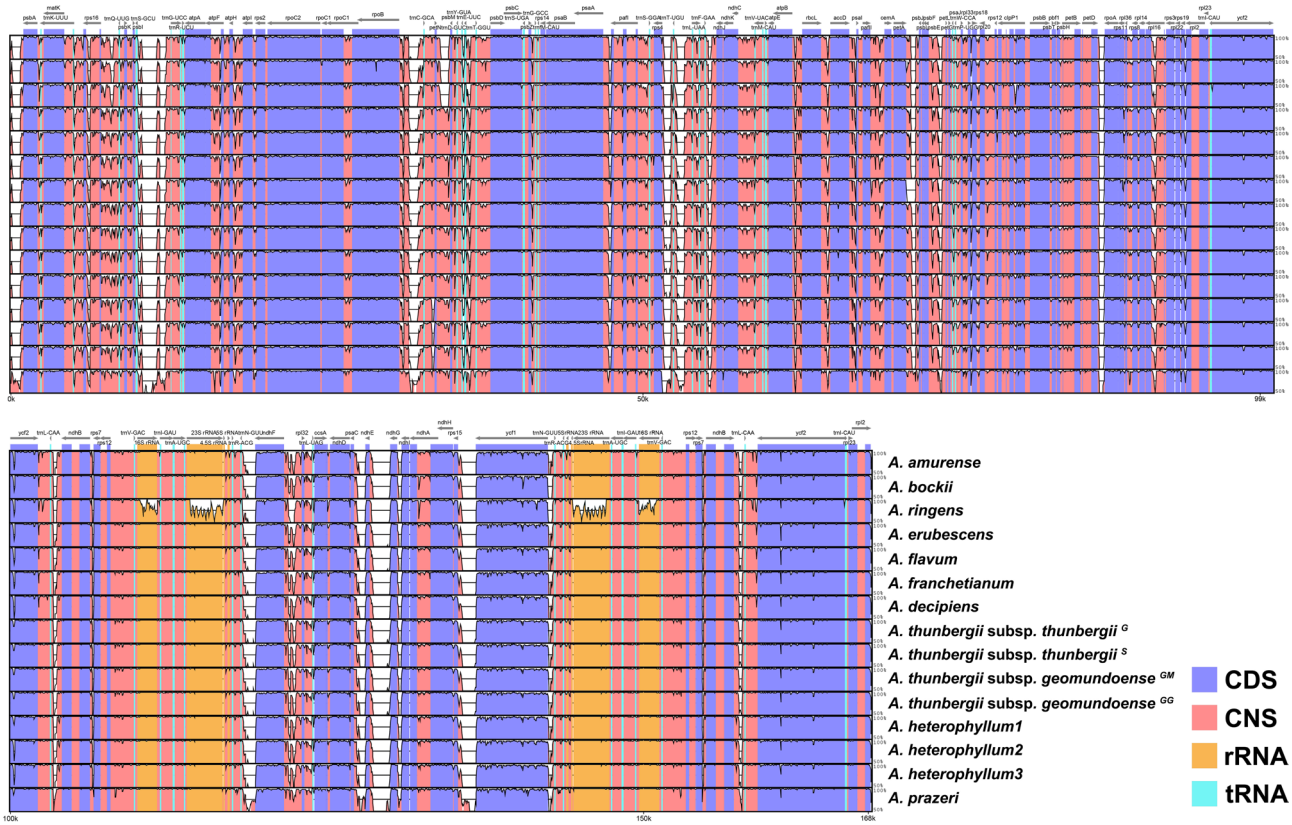

Fig. 2. Percent sequence identity plots of plastomes from 15 *Arisaema* taxa, with *Pinellia pedatisecta* Schott (GenBank accession No. OR772809) as the reference. Sequence identity values were calculated and visualized using mVISTA. Superscript abbreviations denote sampling localities; *GG* Gageodo Island individual, *GM* Geomundo Island individual, *G* Gyoraeri Natural Recreation Forest individual, *S* Seogwipo Natural Recreation Forest individual.

for isoleucine, I) was the most frequently used codon (966–976), whereas UGC (coding for cysteine, C), was the least used (59–64). For RSCU values, the CUU (coding for leucine, L) exhibited the highest values (1.806–1.838; mean 1.822), whereas the AGC (coding for serine, S) had the lowest values (0.351–0.370; mean 0.362). Notably, in *A. thunbergii* (including *A. thunbergii* subsp. *geomundoense*), GGC (coding for glycine, G) was the least preferred codon, with RSCU values of 0.375–0.376. The codons AUG (coding for methionine, M) and UGG (coding for tryptophan, W) both showed RSCU values of 1.

Identified molecular diagnostic characters in *Arisaema*

We aligned 78 plastid PCGs across all Aroideae taxa and identified molecular diagnostic characters (MDCs) counts of 177 in *Arisaema* (including 9 deletions), 77 in *Sauromatum*, 188 in *Typhonium* (with 6 insertions and 9 deletions), and 205 in *Pinellia* (with 12 insertions and 6 deletions) (Fig. 6 and Table S4). A focused analysis within *Arisaema* revealed sect. *Pistillata* to possess 47 unique MDCs, sect. *Sinarisaema* 8, sect. *Dochafa* 17, sect. *Franchetiana* 91 (including 18 insertions), sect. *Decipientia* 131 (including 12 insertions and 42 deletions), sect. *Flagellarisaema* 79 (including 9 insertions), and sect. *Odorata* 403 (including 57 insertions and 48 deletions). MDCs were detected using two separate alignments: one comprising all Aroideae species and another limited to *Arisaema* species.

Phylogenetic relationships of *Arisaema*

An alignment matrix consisting of 78 plastid PCGs from 19 ingroup and three outgroup taxa contained 68,988 characters, of which 65,971 (95.63%) were constant and 1,451 (2.10%) were parsimony-informative. Maximum parsimony (MP) analysis Yielded the most parsimonious tree with a length of 3,488, a consistency index (CI) of 0.904, and a retention index (RI) of 0.930. The topologies inferred from MP, maximum likelihood (ML), and Bayesian inference (BI) analyses were largely congruent, with strong support at most nodes: parsimony bootstrap percentages (PBP) exceeding 90%, mean bootstrap percentages (MBP) reaching 95%, SH-like approximate likelihood ratio test (SH-aLRT) values of 95%, and posterior probabilities (PP) of 0.95 or higher. Within *Arisaema*, seven sections were recovered as monophyletic. Sect. *Odorata* (*A. prazeri* Hook.f.) formed a basal clade (PBP = 100; MBP = 100; SH-aLRT = 100; PP = 1.00), followed by the divergence of sect. *Flagellarisaema*, which includes the focal species of this study, *A. thunbergii* and *A. heterophyllum* (PBP = 100; MBP = 100; SH-aLRT = 100; PP = 1.00). However, the subspecies of *A. thunbergii* were not fully resolved, forming a polytomy

Fig. 3. Circular map of comparative plastome analyses in *Arisaema* generated with CGView, using *A*. *prazeri* Hook.f. as the reference. Outer ring shows annotated genes (CDS in blue, tRNA in red, rRNA in purple); genes outside the ring are Transcribed counter-clockwise, inside clockwise. The innermost ring marks the 50 kb scale of the *A*. *prazeri* plastome; the second innermost ring shows GC skew [(G–C)/(G + C)], with positive skew in green and negative skew in purple; the third innermost ring shows GC content (%) in 100 bp windows.

in both MP and BI trees (Fig. 7). Among the five remaining sections, sect. *Pistillata* was resolved as sister to the clade comprising sect. *Dochafa* and sect. *Sinarisaema*, forming a terminal group with moderate support (PBP = 76; MBP = 76; SH-aLRT = 74.2; PP = 0.9321).

Divergence time estimation of *Arisaema*

The mean divergence age estimates and 95% highest posterior density (HPD) intervals for key nodes from the BEAST analysis are presented in Fig. 8; Table 2. The results suggest that *Arisaema* diverged during the Oligocene, approximately 27.29 million years ago (Mya), with a 95% HPD range of 24.10–30.36 (node 1). *Arisaema* sect. *Odorata* diverged around 18.81 Mya (95% HPD: 14.32–23.43 Mya, node 2), while sect. *Flagellarisaema* diverged approximately 14.47 Mya (95% HPD: 10.30–18.73 Mya, node 3). The subsequent split between the *A*. *thunbergii* individuals and *A*. *heterophyllum* occurred around 7.61 Mya, with a 95% HPD range of 3.58–11.84 Mya (node 4). Sect. *Decipientia* diverged approximately 10.21 Mya (95% HPD: 6.85–13.64 Mya, node 5), while sect. *Franchetiana* split around 8.89 Mya (95% HPD: 5.85–11.98 Mya, node 6). Among the remaining sections, sect. *Pistillata* and sect. *Sinarisaema* + sect. *Dochafa* diverged around 8.50 Mya, with a 95% HPD range of 5.60–11.58 Mya (node 7).

Discussion

Plastome structure of *Arisaema* and comparative analyses

In recent studies, plastome sequences of *Arisaema* were reported[27–29] but structural variations among species were not analyzed. We completed plastome sequencing for five *Arisaema* taxa classified within sect. *Flagellarisaema*. As with most species in the subf. Aroideae, the *inf*A gene, which encodes Translation initiation factor 1 and

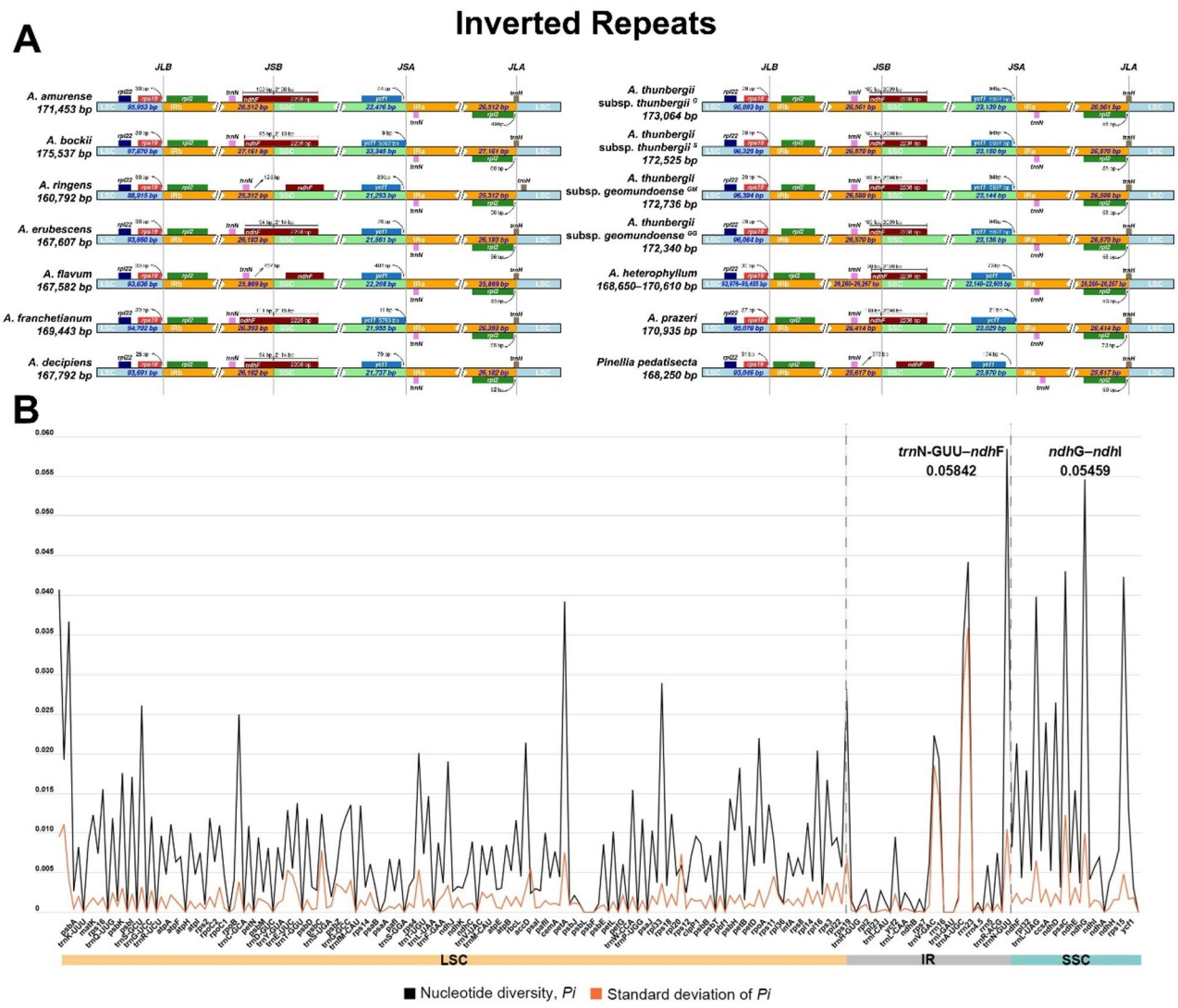

Fig. 4. (**A**) Comparison of the large single-copy (LSC), small single-copy (SSC), and inverted repeat (IR) region boundaries; (**B**) nucleotide diversity (*Pi*) across the plastomes across the 15 *Arisaema* plastomes, calculated for protein-coding genes (PCGs), tRNA, rRNA, and intergenic regions using a sliding-window analysis (window = 100 bp and step = 25 bp). Superscript abbreviations denote sampling localities; *GG* Gageodo Island individual, *GM* Geomundo Island individual, *G* Gyoraeri Natural Recreation Forest individual, *S* Seogwipo Natural Recreation Forest individual.

participates in the assembly of the initiation complex, was universally pseudogenized across all examined *Arisaema* species[25,30–33]. This was determined by detecting an open reading frame (ORF) with a conserved domain via the NCBI Conserved Domains Database (CDD), following the approach of Wang et al.[34]. In some angiosperms, *inf*A has relocated from the plastome to the nucleus, likely due to relaxed purifying selection on the plastome[35].

Our comparative analyses indicate that the plastomes of *A. thunbergii* subsp. *geomundoense* and its closest relatives are highly conserved in structure. In contrast, *A. ringens* exhibits markedly elevated nucleotide diversity in the 16 S and 23 S rRNA genes (Figs. 2 and 3), resulting in increased *Pi* values within the IR regions (Fig. 4B). This finding deviates from the common pattern observed in angiosperms, where IR regions typically display lower variability than the LSC and SSC regions[36,37]. Moreover, in *A. ringens*, the *trn*H-GUG gene is situated entirely within the LSC region, whereas in other *Arisaema* taxa, it spans the boundary between the LSC and IR regions. Since tRNA and rRNA genes are typically well conserved in other angiosperms, including other *Arisaema* taxa, further studies are required to confirm these variations across different individuals of *A. ringens*. We also calculated the standard deviation of *Pi* (Fig. 4B), which supported the expected patterns: high *Pi* with low standard deviation reflects uniformly high diversity, high *Pi* with high standard deviation indicates localized peaks of variability, and low *Pi* with high standard deviation reveals isolated clusters of variation within otherwise conserved regions. Altogether, these results strongly support the hypothesis that *A. ringens* alone underlies the elevated diversity.

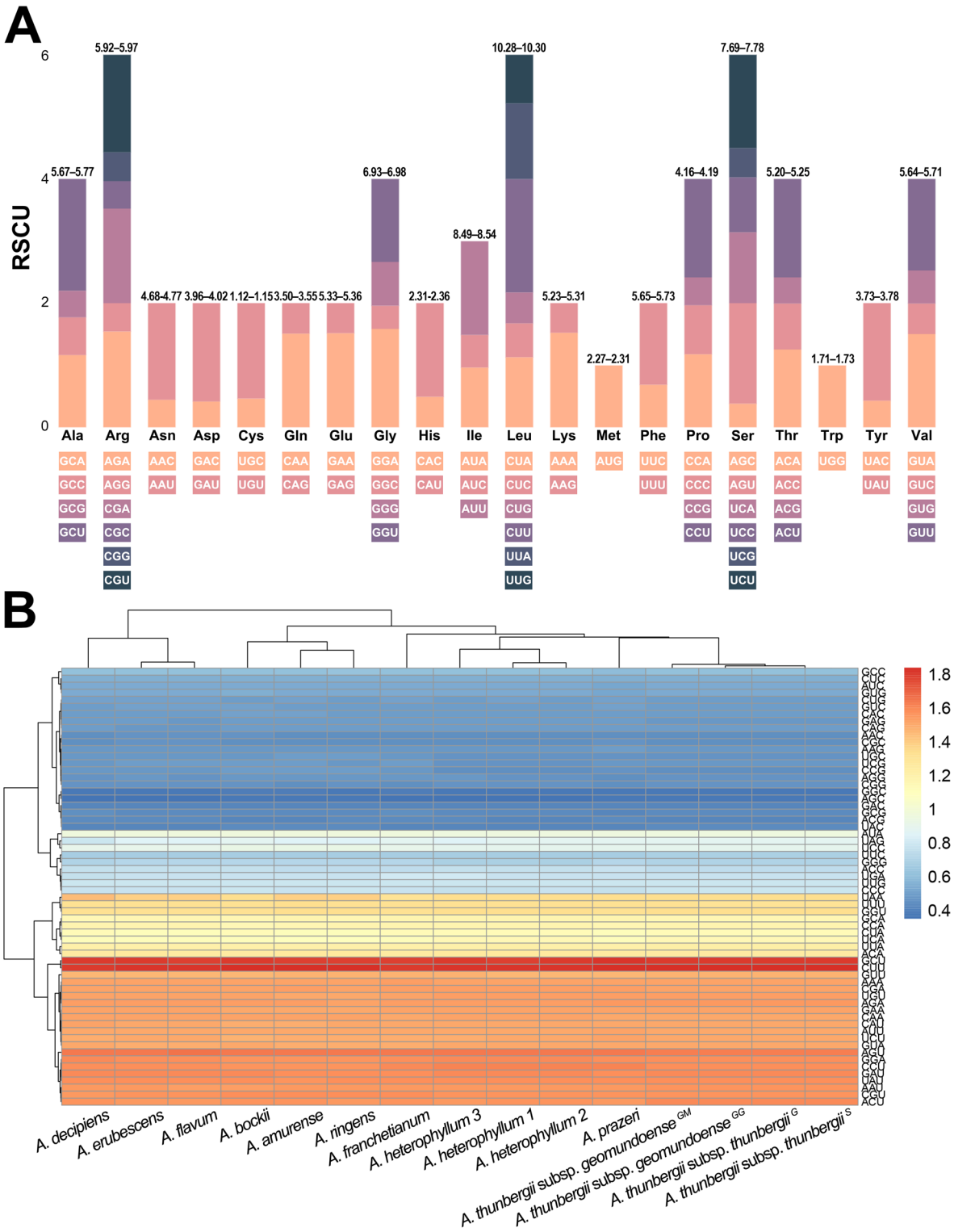

Fig. 5. Relative synonymous codon usage (RSCU) analysis of 20 amino acids across 78 plastid protein-coding genes (PCGs) in 15 *Arisaema* plastomes. (**A**) Stacked-bar chart displaying the RSCU values for each amino acid, with frequencies indicated above each bar; (**B**) Heat map of codon usage bias, where red denotes higher RSCU values and blue denotes lower RSCU values.

Finally, codon usage analysis of the 78 plastid PCGs indicates that both mutational bias and selection influence species-level codon frequencies: codons ending in A or U are preferentially used, while those ending in G or C are underrepresented. Similar patterns have been reported in other Aroideae taxa[38] underscoring the value of RSCU studies for uncovering evolutionary processes. Unlike other *Arisaema* taxa, *A. thunbergii* (including *A.*

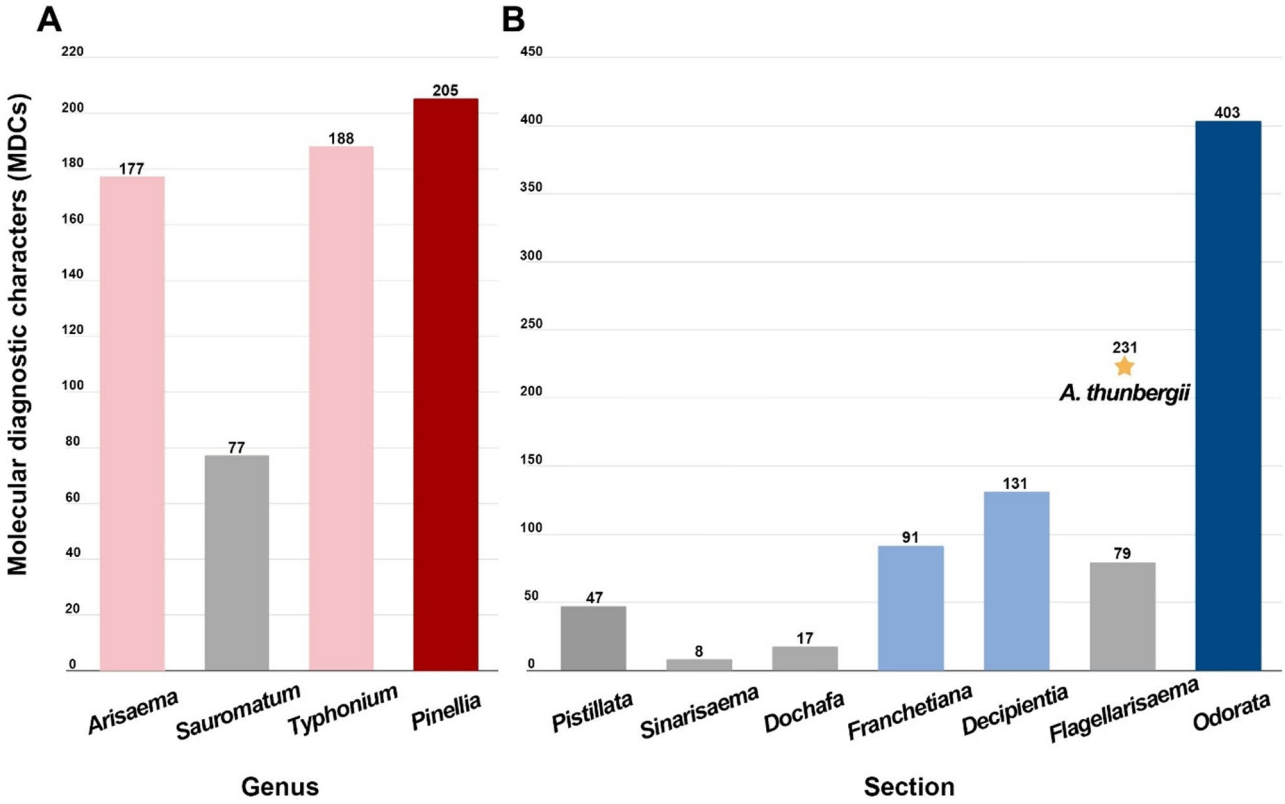

Fig. 6. Assessment of molecular diagnostic characters (MDCs) across 78 plastid protein-coding genes (PCGs). (**A**) MDC counts across 22 Aroideae species. (**B**) MDC counts across 15 *Arisaema* taxa, grouped by section. Red and blue bars represent more than 200 MDCs; pink and sky-blue bars represent 80–200 MDCs; and gray bars represent fewer than 80 MDCs.

thunbergii subsp. *geomundoense*) exhibited its lowest RSCU value for the GGC codon rather than for AGC (Table S3). This atypical bias may reflect lineage-specific shifts in translational selection or genome composition. For instance, it could influence the efficiency of glycine incorporation during protein synthesis or signal adaptive responses to ecological pressures unique to *A. thunbergii*. Further investigation of gene expression levels and tRNA abundances in this species will help clarify the functional consequences of this codon usage deviation.

Putative molecular markers in *Arisaema* and related genera

Recently, MDCs have been utilized to distinguish cultivars and as evidence for taxonomic treatments[39]. Although the sampling was not sufficient to cover the entire genus, we analyzed the unique MDCs present in *Arisaema*, *Sauromatum*, *Typhonium*, and *Pinellia* of the subfamily Aroideae, as well as the MDCs in different sections within the genus *Arisaema* (Fig. 6 and Table S4). Among the four genera analyzed in this study, we identified 177 MDCs unique to *Arisaema*, including 3 insertions and 9 deletions. We also identified a total of 33 MDCs in the *ycf*1, and the gene with the highest MDC density relative to its length was *psb*K (total length: 189 bp, 2 MDCs, and MDC density: 1.058). Notably, *Arisaema* sect. *Odorata*, which is positioned in the basal group of the genus, exhibited the highest number of MDCs (Fig. 6). In our target taxon, *A. thunbergii* (including *A. thunbergii* subsp. *geomundoense*), we found 231 unique MDCs, among which 167 were insertions in the *acc*D (MDC density: 9.565). The next highest number was found in the *atp*B, with 9 MDCs and a density of 0.601, of which 6 were deletions resulting in the loss of 'DT' amino acids. These findings are expected to be useful for the future development of super-barcoding systems or molecular markers based on the unique genetic characteristics of *Arisaema* and its sections.

Phylogenetic position of *A. thunbergii* subsp. *geomundoense* and its taxonomic revision

The genus *Arisaema* is well classified into 15 sections and has been extensively studied in terms of its phylogenetic relationships and biogeographical history, despite its morphological diversity[19,40]. Our phylogenetic analyses indicated that seven sections within *Arisaema* were monophyletic, with *A. prazeri* from the sect. *Odorata* identified as the basal lineage of the genus. High support values were observed at almost all nodes, except for the relationship between sect. *Pistillata* and the clade comprising sect. *Dochafa* and sect. *Sinarisaema* (PBP = 76; MBP = 76; SH-aLRT = 74.2; PP = 0.9321) (Fig. 7). Compared with the phylogenetic relationships inferred from the data of Tran et al.[40], our dataset, although lacking many *Arisaema* species, shows that monotypic sect. *Dochafa* [*A. flavum*] clusters with sect. *Sinarisaema*, forming a terminal clade. In contrast, in the phylogeny

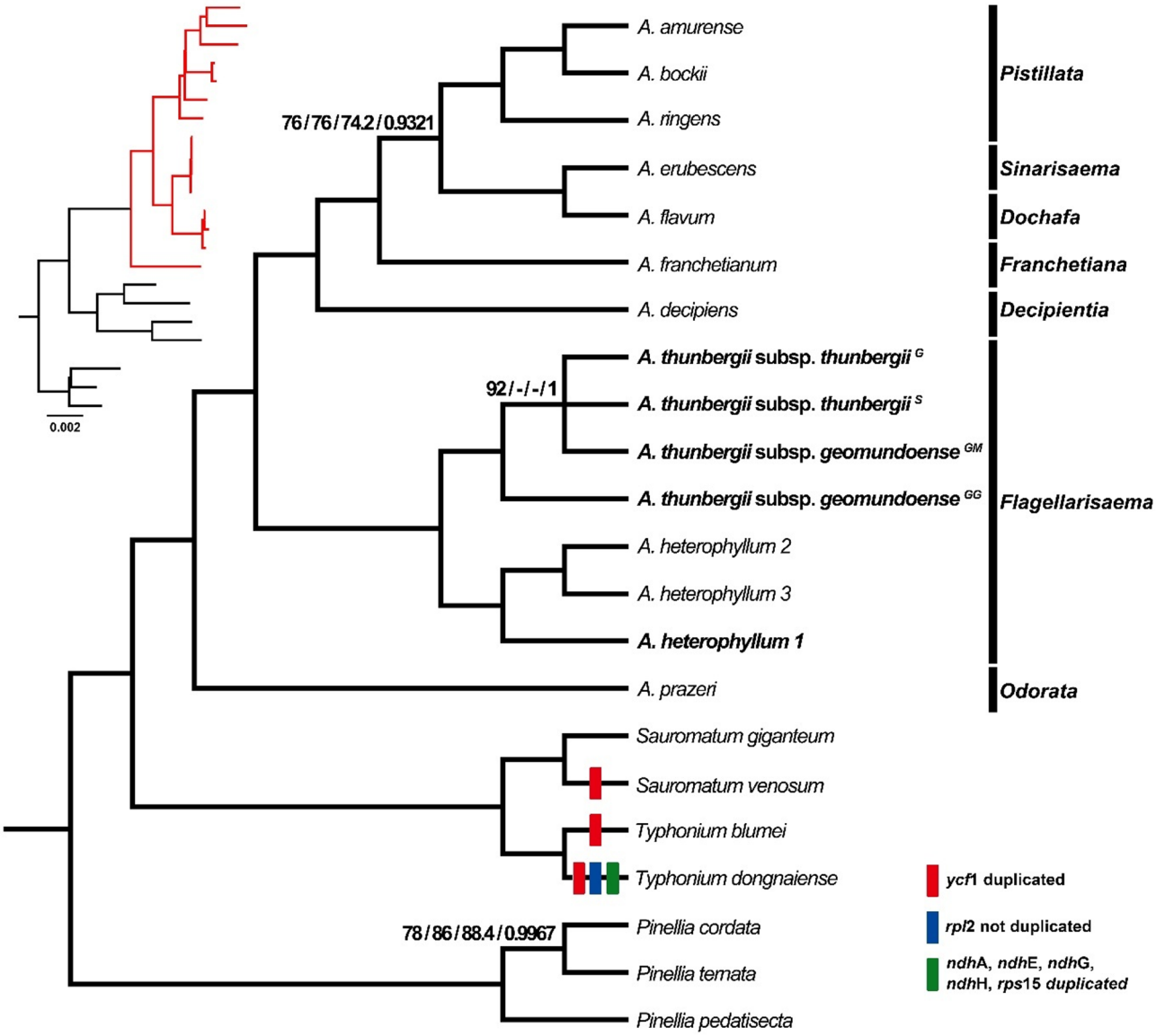

Fig. 7. Strict consensus tree derived from 78 plastid protein-coding genes (PCGs). Support at each node is indicated as parsimony bootstrap percentage (PBP)/mean bootstrap percentage (MBP)/SH-like approximate likelihood ratio test support (SH-aLRT)/posterior probability (PP). Only nodes with PBP ≤ 95%, MBP ≤ 95%, SH-aLRT ≤ 95%, and PP ≤ 0.95 are annotated; nodes failing to meet any of these criteria or displaying conflicting topologies are marked "–". Taxa sequenced in this study are shown in bold, and boxes indicate sectional placement within *Arisaema*. Colored boxes indicate genomic events identified from the complete plastomes. Superscript abbreviations denote sampling localities; *GG* Gageodo Island individual, *GM* Geomundo Island individual, *G* Gyoraeri Natural Recreation Forest individual, *S* Seogwipo Natural Recreation Forest individual.

of Tran et al.[40], sect. *Dochafa* did not form a terminal clade but instead diverged shortly after the basal clade comprising sect. *Fimbriata*, *Odorata*, *Attenuata*, and *Anomala*.

The Korean endemic plant *A. thunbergii* subsp. *geomundoense* was first described by Ko et al.[20] and is distinguished by a dark, wrinkled enlargement at the base of spadix appendage (Fig. 1). This subspecies has been continuously identified and reported in the northern island regions of Korea[41,42]yet its phylogenetic relationship with *A. thunbergii* subsp. *thunbergii* remains unclear due to limited research. Noh et al.[22] conducted the first genetic analysis of Korean *Arisaema* species using three DNA barcodes (plastid *mat*K and *rbc*L and nuclear ITS), including both *A. thunbergii* subsp. *geomundoense* and *A. thunbergii* subsp. *thunbergii*. Their results revealed no genetic variation between the two subspecies, indicating that they form a single cluster. Similarly, our phylogenetic analyses based on both the MP and BI analyses also showed that *A. thunbergii* subsp. *thunbergii* and *A. thunbergii* subsp. *geomundoense* form a polytomy, further supporting their genetic indistinguishability. In

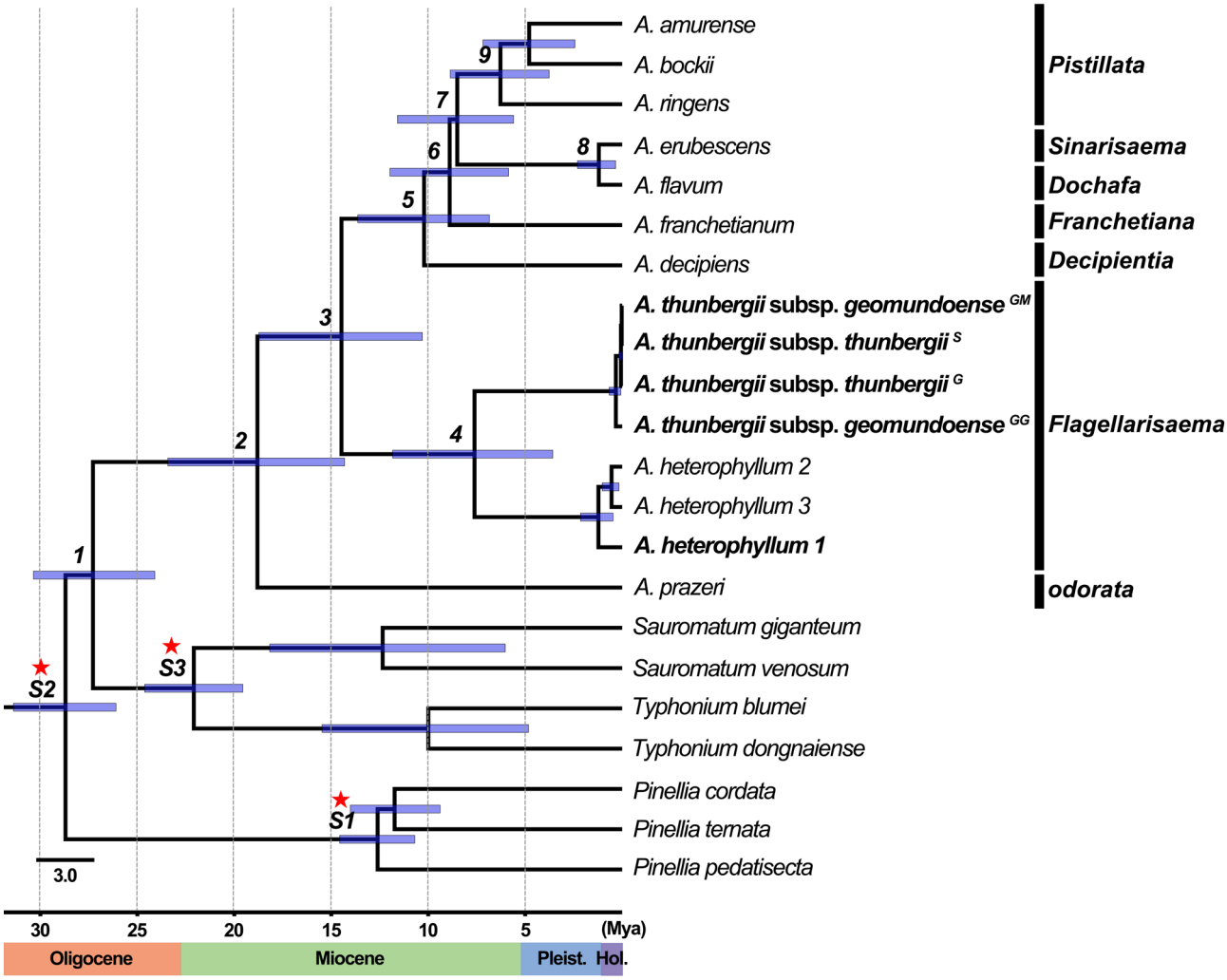

Fig. 8. Chronogram of *Arisaema* inferred from 78 plastid protein-coding genes (PCGs) using BEAST. Nodes indicate posterior mean ages, and blue bars represent 95% highest posterior density (HPD) intervals. Numbers 1–9 correspond to nodes of interest (Table 2). Calibration points S1–S3 are marked with red stars. Geological epochs are shown along the time axis beneath the tree. Superscript abbreviations denote sampling localities; *GG* Gageodo Island individual, *GM* Geomundo Island individual, *G* Gyoraeri Natural Recreation Forest individual, *S* Seogwipo Natural Recreation Forest individual.

Node	Description	Age estimate	
		Mean (Mya)	95% HPD (Mya)
1	Genus *Arisaema* (stem node)	27.29	24.10–30.36
2	Genus *Arisaema* (crown node)	18.81	14.32–23.43
3	Sect. *Flagellarisaema* (stem node)	14.47	10.30–18.73
4	Sect. *Flagellarisaema* (crown node)	7.61	3.58–11.84
5	Sect. *Decipientia* (stem node)	10.21	6.85–13.64
6	Sect. *Franchetiana* (stem node)	8.89	5.85–11.98
7	Sect. *Pistillata* (stem node)	8.50	5.60–11.58
8	Sect. *Sinarisaema* + *Dochafa* (crown node)	1.20	0.34–2.30
9	Sect. *Pistillata* (crown node)	6.28	3.76–8.87

Table 2. Estimated divergence times within *Arisaema*.

both studies, the subspecies of *A. thunbergii* clustered with *A. heterophyllum*, a member of sect. *Flagellarisaema*, which was consistently recovered as a monophyletic group.

According to the recent data from Plants of the World Online[43]*A. thunbergii* subsp. *geomundoense* is treated as a synonym of *A. thunbergii* subsp. *urashima* (H.Hara) H.Ohashi & J.Murata. However, this classification conflicts with the identification key proposed by Ko et al.[20], which specifically distinguishes *A. thunbergii* subsp. *geomundoense* by its smooth yet wrinkled enlargement at the base of the spadix appendage. To clarify this ambiguous classification, we collected two individuals from each subspecies, *A. thunbergii* subsp. *geomundoense* and *A. thunbergii* subsp. *thunbergii*. Our plastome analyses revealed that *A. thunbergii* subsp. *geomundoense* collected from Geomundo Island, where the paratype specimens were originally obtained, had identical plastid PCGs to *A. thunbergii* subsp. *thunbergii*, indicating no genetic differentiation. In addition, comparative plastome analyses showed no structural variation among the subspecies of *A. thunbergii*. These findings strongly suggest that *A. thunbergii* subsp. *geomundoense* should be treated as a synonym of *A. thunbergii* subsp. *thunbergii*, warranting a taxonomic reassessment of its subspecific status. Moreover, the morphological characteristics proposed by Ko et al.[20], such as the color and wrinkling of the enlargement at the base of spadix appendage, are likely the result of ecological variation rather than genetic differentiation. To further clarify infraspecific classification within *A. thunbergii*, additional research on the Japanese subspecies, *A. thunbergii* subsp. *urashima*, is necessary.

Divergence times of *Arisaema*

The divergence times of *Arisaema* have been reported in previous studies[15,21,40,44,45]. Although our analysis included fewer *Arisaema* species and did not incorporate fossil data, our results suggest seven sectional divergence events based on genomic data. Using a dataset of 78 plastid PCGs, the stem node of *Arisaema* was estimated at 27.29 Mya, with a 95% HPD of 24.10–30.36 Mya. This estimate is younger than those reported by Nauheimer et al.[45] (approximately 32 Mya) and Tran et al.[40] (33.27 Mya), but similar to the estimate by Zhao et al.[15] (approximately 28 Mya). Divergence time estimation is known to be influenced by factors such as taxon sampling and the type of genetic data used; however, fossil calibrations typically have a greater impact on the resulting estimates[46,47]. While Tran et al.[40] analyzed 127 *Arisaema* species using a single fossil calibration and four chloroplast DNA regions, our study followed a more recent approach that employed five fossil calibrations and transcriptome data[15]. Based on our results, the genus *Arisaema* likely began diverging in the late Oligocene, followed by subsequent sectional diversification events throughout the Miocene.

Conclusions

We present a well-supported phylogenetic framework for the genus *Arisaema* using complete plastome sequences. Since our study focused on verifying the taxonomic status of the Korean endemic *A. thunbergii* subsp. *geomundoense*, sampling was concentrated within the sect. *Flagellarisaema*. Although this Limited the resolution of relationships among all 15 sections in *Arisaema* based on genomic data, our results indicate that *Arisaema* exhibits conserved plastome structures. Moreover, the MDCs identified in this study offer additional genetic resources that can facilitate super-barcoding and enable high resolution taxonomic identification within *Arisaema*. Furthermore, plastome analyses support the treatment of *A. thunbergii* subsp. *geomundoense* as a synonym of *A. thunbergii* subsp. *thunbergii*. Expanding the dataset to include Japanese *A. thunbergii* subsp. *thunbergii* and *A. thunbergii* subsp. *urashima* would enhance their subspecific classification and support research on morphological variations influenced by ecological factors.

Materials and methods

Sample preparation and plastome assembly

Two individuals of *A. thunbergii* subsp. *geomundoense* were collected from natural habitats in South Korea. One was obtained from Geomundo Island, Samsan-myeon, Yeosu-si, Jeollanam-do (N 34°00'30.5" E 127°19'18.9"), the designated location of the paratype[20]while the other was collected from Gageodo Island, Heuksan-myeon, Shinan-gun, Jeollanam-do (N 34°04'45.1" E 125°06'53.1") (Fig. 1). For comparative purposes, additional samples were collected, including two individuals of *A. thunbergii* subsp. *thunbergii* from Gyoraeri Natural Recreation Forest (N 33°26'17.5" E 126°39'49.0") and Seogwipo Natural Recreation Forest (N 33°19'05.2" E 126°28'06.4") on Jeju Island, as well as one individual of *A. heterophyllum* from Mt. Cheonggye in Gyeonggi-do (N 37°23'54.6" E 127°02'25.5").

Leaf tissues were were silica-dried prior to genomic DNA (gDNA) extraction, and corresponding voucher specimens were prepared and archived in the Gachon University Herbarium (GCU) (Table 1). Total gDNA was extracted from the dried material using a modified cetyltrimethylammonium bromide (CTAB) protocol[48]. Plastome sequencing was performed by generating 300 bp paired-end reads on the Illumina MiSeq platform (Table S5). Reads were assembled with reference to the *A. heterophyllum* plastome (GenBank accession No. ON060885) retrieved from NCBI, employing both Geneious Prime 2024.0.5 and GetOrganelle[49,50]. Gene annotation was conducted using GeSeq[51] and the complete plastome was visualized with OGDraw[52].

Comparative analysis of plastome structure and codon usage patterns

The structure, gene content, and organization of the plastomes were analyzed and compared (Table 1). To explore structural variations within *Arisaema*, 12 previously published plastome sequences were incorporated into the analysis (Table S6). Whole plastome sequences were aligned using MUSCLE and visualized with the LAGAN mode in mVISTA[53,54]. For the mVISTA visualization, the annotated plastome sequences of *Pinellia pedatisecta* Schott (GenBank accession No. OR772809) was selected as the reference due to its sister-group relationship with *Arisaema*, enabling assessment of sequence conservation and divergence at a broader inter-generic scale.

Furthermore, to facilitate structure-focused comparisons within *Arisaema*, we selected the high-quality, well-annotated plastome of *A. prazeri* as the reference and compared it against nine other *Arisaema* plastomes using the CGView Comparison Tool[55]. GC distribution was evaluated by calculating GC skew, defined as (G − C)/(G + C). The IR/LSC and IR/SSC junctions were examined and visualized using IRscope[56].

We evaluated nucleotide diversity (*Pi*) in plastid PCGs, tRNA genes, rRNA genes, and intergenic spacers using data from 15 complete *Arisaema* plastome sequences. Sequence divergence was investigated via a sliding-window analysis in DnaSP v6.0[57], using a 100 bp window and a 25 bp step. Furthermore, the relative synonymous codon usage (RSCU) for 78 plastid PCGs was determined with the DAMBE program[58]. Finally, the RSCU clustering diagram was generated using the pheatmap pacage in R (https://CRAN.R-project.org/package=pheatmap).

Molecular diagnostic characters

Plastid PCGs were analyzed with FastaChar v0.2.4[59] to identify MDCs specific to each *Arisaema* section and unique to the genus in comparison with three related genera.

Phylogenetic analyses

Complete plastome sequences for three *Pinellia* species, *P. cordata* N.E.Br., *P. pedatisecta*, and *P. ternata* (Thunb.) Makino) were downloaded from NCBI to function as outgroups. The ingroup consisted of 15 *Arisaema* taxa, along with two species each from *Sauromatum* and *Typhonium*, to reconstruct phylogenetic relationships. For phylogenetic analysis, we extracted 78 plastid PCGs and aligned them using MUSCLE in Geneious Prime 2024.0.5[49]. Then, we inferred the phylogeny using MP, ML, and BI approaches. MP analysis was carried out in PAUP* v4.0a[60], with all characters equally weighted and unordered and gaps treated as missing. A heuristic search employed 1,000 random addition replicates combined with tree bisection and reconnection (TBR) branch swapping, retaining up to ten most-parsimonious trees per replicate. Clade support was assessed via 1,000 bootstrap pseudoreplicates under the same settings, reported as PBP. ML inference was performed on the IQ-TREE web server (http://iqtree.cibiv.univie.ac.at/), with node support quantified by MBP and SH-aLRT based on 10,000 ultrafast bootstrap. Appropriate substitution models were selected and applied to each gene (Table S7). For BI, the optimal nucleotide substitution model was selected in MEGA 11 using the Bayesian Information Criterion (BIC; Table S8)[61]. MrBayes v3.2.7[62] analyses consisted of two independent runs of 1 million generations, sampling every 1,000 generations. The initial 25% of samples were discarded as burn-in, and a 50% majority-rule consensus tree was generated from the remaining trees, with PP providing branch support. Convergence was confirmed by ensuring all parameters achieved an effective sample size (ESS) greater than 200. Finally, phylogenetic trees were visualized and edited in FigTree v1.4.4[63].

Molecular dating

Divergence times within *Arisaema* were inferred using BEAST v1.10.4[64], drawing on 78 plastid PCGs. BEAUti v1.10.4 was employed to construct the input XML, specifying a GTR + I + G substitution model, identical to that used in our BI, a Yule speciation prior, and an uncorrelated lognormal relaxed clock[65,66]. The Markov chain Monte Carlo (MCMC) chain ran for 100 million generations, with samples taken every 1,000 generations. After discarding the first 10% of trees as burn-in, the remaining trees were summarized into a maximum clade credibility chronogram in TreeAnnotator v1.10.4, using mean node heights and a posterior probability cutoff of 0.50. Mean divergence estimates and their 95% HPD intervals were extracted in Tracer and visualized in Figtree v1.4.4[63].

In the absence of fossil constraints for both our ingroup and outgroup, we employed three secondary calibration priors: the *Pinellia* crown node was estimated at 13 Mya with a normal distribution (mean = 13 and standard deviation = 1; S1)[67]the *Pinellia* stem node at 28 Mya with a normal distribution (mean = 28 and standard deviation = 1.5; S2)[15]and the *Sauromatum* + *Typhonium* crown node at 23 Mya with a normal distribution (mean = 23 and standard deviation = 1.5; S3)[68]. These priors were incorporated to improve the precision of our divergence time estimates.

Data availability

The five plastome sequences we obtained from this study were archived in NCBI. The accession numbers are presented in Table 1 (PV231676–PV231680).

Received: 30 April 2025; Accepted: 11 September 2025
Published online: 15 October 2025

References

1. Kim, Y. et al. Plastome-based backbone phylogeny of East Asian *Phedimus* (Subgenus *Aizoon*: Crassulaceae), with special emphasis on Korean endemics. *Front. Plant Sci.* **14**, 1089165 (2023).
2. Park, S. & Park, S. Large-scale phylogenomics reveals ancient introgression in Asian *Hepatica* and new insights into the origin of the insular endemic *Hepatica maxima*. *Sci. Rep.* **10**, 16288 (2020).
3. Nakai, T. A. Synoptical Sketch of Korean Flora. *Bull. Natl. Sci. Mus.* **94**, 63 (1952).
4. B Lee, T. Korea-Japan joint symposium on plant taxonomy: outline of Korean endemic plants and their distribution. *Korean J. Plant. Taxonomy*. **14**, 21–32 (1984).
5. Paik, W. K. The status of endemic plants in Korea and our tasks in the 21st century. *Korean J. Plant. Taxonomy*. **29**, 263–274 (1999).
6. Kim, M. Y. *Korean Endemic Plants*. (Solkwahak, 2004).
7. Oh, B. Endemic vascular plants in the Korean peninsula. *Korea Natl. Arboretum* **205**, 97 (2005).
8. Chung, G. Y. et al. A checklist of endemic plants on the Korean Peninsula. *Korean J. Plant. Taxonomy*. **47**, 264–288 (2017).
9. Chung, G. Y. et al. A checklist of endemic plants on the Korean Peninsula II. *Korean J. Plant. Taxonomy*. **53**, 79–101 (2023).

10. Mayo, S., Bogner, J. & Boyce, P. in *Flowering Plants· Monocotyledons: Alismatanae and Commelinanae (except Gramineae)* 26–74Springer, (1998).
11. Gusman, G. & Gusman, L. The genus *Arisaema*: a monograph for botanists and nature lovers. *(No Title)* (2006).
12. Bogner, J. & Hesse, M. Zamioculcadoideae, a new subfamily of Araceae. *Aroideana: J. Int. Aroid Soc.* **28**, 3–20 (2005).
13. Cabrera, L. I. et al. Phylogenetic relationships of aroids and duckweeds (Araceae) inferred from coding and noncoding plastid DNA. *Am. J. Bot.* **95**, 1153–1165 (2008).
14. Henriquez, C. L., Arias, T., Pires, J. C., Croat, T. B. & Schaal, B. A. Phylogenomics of the plant family Araceae. *Mol. Phylogenet. Evol.* **75**, 91–102 (2014).
15. Zhao, L. et al. Phylotranscriptomic analyses reveal multiple whole-genome duplication events, the history of diversification and adaptations in the Araceae. *Ann. Botany*. **131**, 199–214 (2023).
16. Haigh, A. L. et al. Target sequence data shed new light on the infrafamilial classification of Araceae. *Am. J. Bot.* **110**, e16117 (2023).
17. Kant, K., Lal, U. R., Rawat, R., Kumar, A. & Ghosh, M. Genus *Arisaema*: a review of traditional importance, chemistry and biological activities. *Comb. Chem. High Throughput Screen.* **23**, 624–648 (2020).
18. Murata, J., Nagamasu, H. & Ohashi, H. A nomenclatural review on the infrageneric classifications of *Arisaema* (Araceae). *J. Japanese Bot.* **88**, 36–45 (2013).
19. Ohi-Toma, T., Wu, S., Murata, H. & Murata, J. An updated genus-wide phylogenetic analysis of *Arisaema* (Araceae) with reference to sections. *Bot. J. Linn. Soc.* **182**, 100–114 (2016).
20. Ko, S. C., Lee, D. B., Shin, Y. H. & Tae, K. H. *Arisaema thunbergii* supsp. *geomundoense* SC Ko (Araceae), a new subspecies from Korea. *Korean J. Plant. Taxonomy*. **36**, 209–216 (2006).
21. Renner, S. S., Zhang, L. B. & Murata, J. A chloroplast phylogeny of *Arisaema* (Araceae) illustrates tertiary floristic links between Asia, North America, and East Africa. *Am. J. Bot.* **91**, 881–888 (2004).
22. Noh, P. et al. Study on molecular phylogenetics of Korean *Arisaema* species based on universal DNA barcodes. *Korean J. Plant. Resour.* **31**, 37–51 (2018).
23. Zhou, N. et al. Historical biogeography and evolutionary diversification of *Lilium* (Liliaceae): new insights from plastome phylogenomics. *Plant. Divers.* **46**, 219–228 (2024).
24. Noroozi, M., Ghahremaninejad, F., Riahi, M. & Cohen, J. I. Phylogenomics and plastome evolution of Lithospermeae (Boraginaceae). *BMC Plant Biol.* **24**, 957 (2024).
25. Henriquez, C. L. et al. Evolutionary dynamics of chloroplast genomes in subfamily Aroideae (Araceae). *Genomics* **112**, 2349–2360 (2020).
26. Li, Z. Z., Lehtonen, S. & Chen, J. M. The dynamic history of plastome structure across aquatic subclass Alismatidae. *BMC Plant Biol.* **23**, 125 (2023).
27. Cai, X. L. et al. Complete plastome sequence of *Arisaema ringens* (Araceae): a dioecious herb disjunctly distributed in china, Japan and Korea. *Mitochondrial DNA Part. B*. **4**, 540–541 (2019).
28. Zhang, Y., Guo, X. & Yan, B. Characterization of the complete chloroplast genome of *Arisaema erubescens* (Wall.) schott, a traditional Chinese medicinal herb. *Mitochondrial DNA Part. B*. **5**, 3149–3150 (2020).
29. Yi, S. et al. The complete chloroplast genome of *Arisaema bockii* Engler and its phylogenetic analysis in the family araceae. *Mitochondrial DNA Part. B*. **6**, 3283–3285 (2021).
30. Yun, S. & Kim, H. The complete plastome sequence of *Monstera deliciosa* (Araceae), an ornamental foliage plant. *Mitochondrial DNA Part. B*. **8**, 1301–1305 (2023).
31. Henriquez, C. L. et al. Chloroplast genome evolution in the *Dracunculus* clade (Aroideae, Araceae). *Genomics* **113**, 183–192 (2021).
32. Abdullah et al. Comparison of chloroplast genomes among species of unisexual and bisexual clades of the monocot family Araceae. *Plants* **9**, 737 (2020).
33. Abdullah et al. Complete chloroplast genomes of *Anthurium huixtlense* and *Pothos scandens* (Pothoideae, Araceae): unique inverted repeat expansion and contraction affect rate of evolution. *J. Mol. Evol.* **88**, 562–574 (2020).
34. Wang, J. et al. The conserved domain database in 2023. *Nucleic Acids Res.* **51**, D384–D388 (2023).
35. Millen, R. S. et al. Many parallel losses of *inf*A from chloroplast DNA during angiosperm evolution with multiple independent transfers to the nucleus. *Plant. Cell.* **13**, 645–658 (2001).
36. Nanjala, C. et al. Plastome structure of 8 *Calanthe* s.l. species (Orchidaceae): comparative genomics, phylogenetic analysis. *BMC Plant Biol.* **22**, 387 (2022).
37. Odago, W. O. et al. Analysis of the complete plastomes of 31 species of *Hoya* group: insights into their comparative genomics and phylogenetic relationships. *Front. Plant Sci.* **12**, 814833 (2022).
38. Jia, X. et al. Codon usage patterns and genomic variation analysis of chloroplast genomes provides new insights into the evolution of Aroideae. *Sci. Rep.* **15**, 4333 (2025).
39. Wong, K. H. et al. Characterisation of the complete chloroplast genomes of seven *Hyacinthus orientalis* L. cultivars: insights into cultivar phylogeny. *Horticulturae* **8**, 453 (2022).
40. Tran, V. T. et al. Reconstruction of the evolutionary biogeography reveals the origin and diversification of *Arisaema* (Araceae). *Acta Botanica Brasilica* **36**,253 (2022).
41. Yang, S. G. et al. Floristic study of Gageodo in Korea. *Korean J. Plant. Resour.* **26**, 597–612 (2013).
42. Jang, C. S. et al. Floristic study of Daeheuksando in Korea. *Korean J. Plant. Resour.* **27**, 518–533 (2014).
43. Powo Plants of the world online. Facilitated by the Royal Botanic Gardens, Kew. *Published on the Internet* (2025).
44. Renner, S. S. & Zhang, L. B. Biogeography of the *Pistia* clade (Araceae): based on chloroplast and mitochondrial DNA sequences and Bayesian divergence time inference. *Syst. Biol.* **53**, 422–432 (2004).
45. Nauheimer, L., Metzler, D. & Renner, S. S. Global history of the ancient monocot family Araceae inferred with models accounting for past continental positions and previous ranges based on fossils. *New Phytol.* **195**, 938–950 (2012).
46. Zheng, Y. & Wiens, J. J. Do missing data influence the accuracy of divergence-time Estimation with BEAST? *Mol. Phylogenet. Evol.* **85**, 41–49 (2015).
47. Hug, L. A. & Roger, A. J. The impact of fossils and taxon sampling on ancient molecular dating analyses. *Mol. Biol. Evol.* **24**, 1889–1897 (2007).
48. Doyle, J. DNA protocols for plants. Molecular techniques in taxonomy. *NATO ASI Ser.* **57**, 283–293 (1991).
49. Kearse, M. et al. Geneious basic: an integrated and extendable desktop software platform for the organization and analysis of sequence data. *Bioinformatics* **28**, 1647–1649 (2012).
50. Jin, J. J. et al. GetOrganelle: a fast and versatile toolkit for accurate de novo assembly of organelle genomes. *Genome Biol.* **21**, 1–31 (2020).
51. Tillich, M. et al. GeSeq–versatile and accurate annotation of organelle genomes. *Nucleic Acids Res.* **45**, 1–11 (2017).
52. Greiner, S., Lehwark, P. & Bock, R. OrganellarGenomeDRAW (OGDRAW) version 1.3. 1: expanded toolkit for the graphical visualization of organellar genomes. *Nucleic Acids Res.* **47**, W59–W64 (2019).
53. Mayor, C. et al. VISTA: visualizing global DNA sequence alignments of arbitrary length. *Bioinformatics* **16**, 1046–1047 (2000).
54. Brudno, M. et al. LAGAN and Multi-LAGAN: efficient tools for large-scale multiple alignment of genomic DNA. *Genome Res.* **13**, 721–731 (2003).
55. Grant, J. R., Arantes, A. S. & Stothard, P. Comparing thousands of circular genomes using the CGView comparison tool. *BMC Genom.* **13**, 1–8 (2012).

56. Amiryousefi, A., Hyvönen, J. & Poczai, P. IRscope: an online program to visualize the junction sites of chloroplast genomes. *Bioinformatics* **34**, 3030–3031 (2018).
57. Rozas, J. et al. DnaSP 6: DNA sequence polymorphism analysis of large data sets. *Mol. Biol. Evol.* **34**, 3299–3302 (2017).
58. Xia, X. & Xie, Z. DAMBE: software package for data analysis in molecular biology and evolution. *J. Hered.* **92**, 371–373 (2001).
59. Merckelbach, L. M. & Borges, L. M. Make every species count: Fastachar software for rapid determination of molecular diagnostic characters to describe species. *Mol. Ecol. Resour.* **20**, 1761–1768 (2020).
60. Swofford, D. L. (2000). PAUP* 4.0, beta version 4.0 b4a. *Sunderland, MA: Sinauer Associates.*
61. Tamura, K., Stecher, G. & Kumar, S. MEGA11: molecular evolutionary genetics analysis version 11. *Mol. Biol. Evol.* **38**, 3022–3027 (2021).
62. Ronquist, F. et al. MrBayes 3.2: efficient bayesian phylogenetic inference and model choice across a large model space. *Syst. Biol.* **61**, 539–542 (2012).
63. Rambaut, A. FigTree–Tree Figure Drawing Tool Version v. 1.4. 4. *Institute of Evolutionary Biology, University of Edinburgh: Edinburgh* (2018).
64. Suchard, M. A. et al. Bayesian phylogenetic and phylodynamic data integration using BEAST 1.10. *Virus evolution* 4, vey016 (2018).
65. Drummond, A. J., Ho, S. Y. W., Phillips, M. J. & Rambaut, A. Relaxed phylogenetics and dating with confidence. *PLoS Biol.* **4**, e88 (2006).
66. Gernhard, T., Hartmann, K. & Steel, M. Stochastic properties of generalised Yule models, with biodiversity applications. *J. Math. Biol.* **57**, 713–735 (2008).
67. Cui, N., Chen, W., Li, X. & Wang, P. Comparative chloroplast genomes and phylogenetic analyses of *Pinellia*. *Mol. Biol. Rep.* **49**, 7873–7885 (2022).
68. Low, S. L. et al. Extensive Miocene speciation in and out of Indochina: the biogeographic history of *Typhonium sensu stricto* (Araceae) and its implication for the assembly of Indochina flora. *J. Syst. Evol.* **59**, 419–428 (2021).

Acknowledgements
The authors would like to thank Shayan Jamshed for collecting the plant material for this study.

Author contributions
JJ collected the plant materials, performed the experiments, analyzed the data, prepared figures and tables, and wrote the initial draft. SS, HOK, and KK performed the experiments, analyzed the data, prepared figures and tables. HJK and JHK designed the experiments and revised the manuscript. All authors agree with the content of the manuscript. All authors have contributed to the manuscript and approved the submitted version.

Funding
This work was supported by grants [KNA1-2-49-25-2] received from the Scientific research of Korea National Arboretum.

Declarations

Competing interests
The authors declare no competing interests.

Ethics approval and consent to participate
The study including plant samples complies with relevant institutional, national, and international guidelines and legislation. No specific permits were required for plant collection. The study did not require ethical approval or consent, as no endangered or protected plant species were involved.

Consent for publication
Not applicable.

Additional information
Supplementary Information The online version contains supplementary material available at https://doi.org/10.1038/s41598-025-20011-y.

Correspondence and requests for materials should be addressed to J.J. or J.-H.K.

Reprints and permissions information is available at www.nature.com/reprints.

Publisher's note Springer Nature remains neutral with regard to jurisdictional claims in published maps and institutional affiliations.

Open Access This article is licensed under a Creative Commons Attribution-NonCommercial-NoDerivatives 4.0 International License, which permits any non-commercial use, sharing, distribution and reproduction in any medium or format, as long as you give appropriate credit to the original author(s) and the source, provide a link to the Creative Commons licence, and indicate if you modified the licensed material. You do not have permission under this licence to share adapted material derived from this article or parts of it. The images or other third party material in this article are included in the article's Creative Commons licence, unless indicated otherwise in a credit line to the material. If material is not included in the article's Creative Commons licence and your intended use is not permitted by statutory regulation or exceeds the permitted use, you will need to obtain permission directly from the copyright holder. To view a copy of this licence, visit http://creativecommons.org/licenses/by-nc-nd/4.0/.

© The Author(s) 2025